A REGION-BASED ALGORITHM FOR BLIND EQUALIZATION OF QAM SIGNALS

João Mendes Filho, Magno T. M. Silva, Maria D. Miranda, and Vítor H. Nascimento

Escola Politécnica, University of São Paulo, São Paulo, SP, Brazil
E-mails: jmendes@lps.usp.br, magno@lps.usp.br, maria@lcs.poli.usp.br, vitor@lps.usp.br

ABSTRACT

We propose a region-based multimodulus algorithm for blind equalization of high-order quadrature amplitude modulation (QAM) signals. It treats nonconstant modulus constellations as constant modulus ones, converging approximately to the Wiener solution. To avoid divergence, it rejects non-consistent estimates of the transmitted signal. When compared to existing blind multimodulus-type algorithms for equalization of QAM signals, it exhibits considerably lower misadjustment, faster convergence, good tracking capability, without compromising the computational cost. Its good behavior is illustrated through simulation results.

***Index Terms*—** Adaptive equalizers, blind equalization, constant modulus algorithm, nonlinearities.

1. INTRODUCTION

The most popular algorithm for blind equalization is the constant-modulus algorithm (CMA). It is well-known that CMA does not solve phase ambiguities introduced by the channel and has a relatively large misadjustment when used to recover nonconstant modulus signals (see, e.g., [1] and the references therein). To jointly recover the modulus and phase of the transmitted signal, the multimodulus algorithm (MMA) was proposed in [2] and [3]. Instead of minimizing the dispersion of the magnitude of the equalizer output, MMA minimizes the dispersion of its real and imaginary parts separately. Thus, it mitigates the intersymbol interference (ISI) and simultaneously corrects the phase rotation, since it implicitly incorporates a phase-tracking loop. Although MMA provides better convergence for high-order QAM signals, it still exhibits a large misadjustment in the steady-state (though smaller than that of CMA).

To overcome the high misadjustment exhibited by CMA and MMA, many algorithms have been proposed in the literature (see, e.g., [4] and the references therein). One of these algorithms, called Sliced MMA (S-MMA), incorporates the sliced symbols (outputs of the decision device) in the multimodulus-based coefficient adaptation process [4]. Although the steady-state misadjustment of S-MMA is much lower than that of MMA for high-order QAM signals, it is still relatively large when compared to the misadjustment obtained in the equalization of constant modulus signals with MMA.

Another algorithm for blind equalization of QAM signals is the soft decision-directed (SDD) algorithm [5]. It is based on the maximization of the *a posteriori* probability density function (pdf) of the equalizer output. To reduce the computational cost, the complex plane of a high-order QAM is divided into a set of regular regions, each with four symbols. Thus, its computational cost is always equivalent to the 4-QAM case, since the pdf of the equalizer output is locally estimated. Its main drawback is that, for a constellation with M symbols, the adaptation process requires $\log_2(M)/2$-stage switchings and each adaptation stage needs a different set of parameters [5]. If the set of parameters is not properly chosen, SDD can suffer from slow convergence and bad tracking capability.

A drawback of all blind algorithms mentioned above is convergence to local minima or even divergence [1]. This can occur when the step-size is not properly chosen or if the initialization is distant from the optimal solution [6]. In order to avoid divergence, dual-mode blind algorithms were recently proposed in [7, 8]. In the first mode, these algorithms work as the normalized CMA [7] or as the Shalvi-Weinstein algorithm [8], while in the second mode, they reject non-consistent estimates of the transmitted signal.

In this paper, we propose a new blind algorithm for equalization of high-order QAM signals that, in addition to the advantages of [4, 5, 7, 8], converges approximately to the Wiener solution, which generally provides a considerably lower misadjustment.

2. PROBLEM FORMULATION AND DM-MMA

Signal $a(n)$ is transmitted through an unknown channel, modeled by a finite impulse response (FIR) filter with impulse response vector $\mathbf{h}^T = [h_0\, h_1\, \cdots\, h_{K-1}]$ and additive white Gaussian noise (AWGN) $\eta(n)$, where the superscript T stands for the transpose of a vector. The received signal $u(n)$ is therefore a distorted version of $a(n)$, corrupted by intersymbol interference and noise. It passes through an FIR filter, whose output is given by $y(n) = \mathbf{u}^T(n)\mathbf{w}(n-1)$, where $\mathbf{u}(n)$, $\mathbf{w}(n-1) \in \mathbb{C}^N$ are the column input regressor and coefficient vectors, respectively. The decision device computes from $y(n)$ a delayed estimate of the transmitted sequence $\hat{a}(n-\Delta)$, Δ being a positive integer. In blind equalization, the algorithms usually update the equalizer coefficients using higher-order statistics of the transmitted signal. Due to its simplicity, CMA is widely used in spite of its slow convergence and possible divergence.

To avoid divergence, a normalized version of CMA was derived in [7]. The algorithm, named DM-CMA, is given by

$$\mathbf{w}(n) = \mathbf{w}(n-1) + \frac{\tilde{\mu}}{\delta + \|\mathbf{u}(n)\|^2}\,[d(n) - y(n)]\,\mathbf{u}^*(n), \quad (1)$$

where $0 < \tilde{\mu} < 2$ is a step-size, δ is a small positive parameter, $(\cdot)^*$ stands for the complex-conjugate, $d(n) = x(n)y(n)$,

$$x(n) = \begin{cases} \big(\beta\sigma_a^2 - |y(n)|^2\big)/\big(\beta\sigma_a^2 - R\big), & \text{if } |y(n)|^2 \le \beta\sigma_a^2 \\ 0, & \text{otherwise,} \end{cases}$$

$\sigma_a^2 = \mathrm{E}\{|a(n)|^2\}$, $R = \mathrm{E}\{|a(n)|^4\}/\mathrm{E}\{|a(n)|^2\}$, $\beta = 2$ (resp., $\beta = 3$) for complex (resp., real) data, and $\mathrm{E}\{\cdot\}$ denotes the expectation operation. It is worth to note that $d(n)$ and $y(n)$ are estimates of the desired response. The consistency between these two estimates will be ensured if $d(n)$ and $y(n)$ have the same sign, which is equivalent to requiring the correction factor $x(n)$ to be always positive. For sub-Gaussian constellations, as is the case for most constellations used in digital communications, the denominator of $x(n)$ is always positive and $x(n) \ge 0$ occurs when $|y(n)|^2 \le \beta\sigma_a^2$. On the other hand, if $|y(n)|^2 > \beta\sigma_a^2$, the algorithm leaves the called *region of interest* and the estimate $d(n)$ is rejected, making $d(n) = 0$.

This work was partly supported by CAPES (scholarship of the institutional quota), CNPq under Grants 302633/2008-1 and 303361/2004-2, and FAPESP under Grants 2008/00773-1 and 2008/04828-5.

This idea can also be extended to ensure the stability of MMA. Using the multimodulus cost function [3], DM-MMA is obtained replacing $d(n)-y(n)$ by $[d_R(n)+jd_I(n)]-[y_R(n)+jy_I(n)]$ in (1), $y_R(n)$ and $y_I(n)$ being the real and imaginary parts of $y(n)$, respectively. The signals $d_R(n)=x_R(n)y_R(n)$ and $d_I(n)=x_I(n)y_I(n)$ depend on the statistics of the real and imaginary parts of the transmitted signals, since

$$x_R(n)=\frac{3\sigma_{a,R}^2-|y_R(n)|^2}{3\sigma_{a,R}^2-R_R},\quad x_I(n)=\frac{3\sigma_{a,I}^2-|y_I(n)|^2}{3\sigma_{a,I}^2-R_I},$$

$\sigma_{a,R}^2=E\{a_R^2(n)\}$, $\sigma_{a,I}^2=E\{a_I^2(n)\}$, $R_R=E\{a_R^4(n)\}/\sigma_{a,R}^2$, and $R_I=E\{a_I^4(n)\}/\sigma_{a,I}^2$. DM-MMA requires $8N+12$ real multiplications ($\times$), $8N+7$ real additions (+), 1 real division ($\div$), and 2 comparisons per iteration.

Through simulations, it was shown in [7] that DM-CMA never diverges. This property can also be extended to DM-MMA. Recently, the same philosophy was applied to the Shalvi-Weinstein algorithm (SWA) in [8]. In this case, assuming the persistence of excitation condition, it was proved through a deterministic analysis that DM-SWA is stable in infinite-precision arithmetic.

3. PROPOSED ALGORITHM

The complex plane is decomposed into a set of $M/4$ minor 4-QAM blocks as in the SDD algorithm of [5]. Each block or regular region A_i contains four symbols, i.e., $A_k=\{a_{km}, m=1,2,3,4\}$, $k=1,2,\ldots,M/4$, where a_{km} takes the value from the M-QAM symbol set. The center of A_k is denoted as $c_k=c_{R,k}+jc_{I,k}$, with $c_{R,k}$ and $c_{I,k}$ the real and imaginary parts of c_k, respectively. With $(\log_2 M-2)$ comparisons, it is possible to identify to which region A_k the sample of the equalizer output belongs.

Variations in the modulus of the transmitted symbol are seen by CMA as a kind of measurement noise [6]. The performance thus can be improved if we trick the algorithm to interpret the input constellation as if it had constant modulus. In order to treat the symbols of the identified region as pertaining to a constant modulus constellation, a translation operation is performed as follows. The center of the identified region is translated to the origin of the complex plane and the rest of the constellation is forgotten. The translation operation works as if the symbols of the translated region $\bar{A}_k$ belonged to a constant modulus 4-QAM constellation. The translated output sample, denoted as $\bar{y}_k=\bar{y}_{R,k}+j\bar{y}_{I,k}=(y_R-c_{R,k})+j\,(y_I-c_{I,k})$, has (by construction, except if y is too large, outside the original constellation) modulus less than or equal to $2\sqrt{2}$, and the translated symbols are given by $\bar{a}_{km}=\pm1\pm j$. Considering both the real and imaginary components of the translated sample apart, the multimodulus cost function with a unitary dispersion constant can be used. As the information of the position of A_k is lost with the translation operation, in order to distinguish the regions, the cost function needs some information about the position of A_k in the complex plane.

To obtain an algorithm which considers the translation operation and the information about the position of A_k, we propose the following instantaneous cost function

$$\hat{J}=\frac{1}{8}\sum_{\ell=1}^{M/4}\alpha_\ell\left[|c_{R,\ell}|[1-\bar{y}_{R,\ell}^2(n)]^2+|c_{I,\ell}|[1-\bar{y}_{I,\ell}^2(n)]^2\right], \quad (2)$$

where $\alpha_\ell=1$ only for the identified region A_k and $\alpha_\ell=0$ for the other $M/4-1$ regions. Note that the multiplication factors $|c_{R,k}|$ and $|c_{I,k}|$ carry the information about the position of A_k. The gradient of $\hat{J}$ is given by [2,3] $\nabla\hat{J}=\sum_{\ell=1}^{M/4}\alpha_\ell\bar{e}_\ell(n)\mathbf{u}^*(n)$, where

$$\bar{e}_\ell(n)=|c_{R,\ell}|\left[\bar{d}_{R,\ell}(n)-\bar{y}_{R,\ell}(n)\right]+j|c_{I,\ell}|\left[\bar{d}_{I,\ell}(n)-\bar{y}_{I,\ell}(n)\right] \quad (3)$$

$$\bar{d}_{R,\ell}(n)=\bar{x}_{R,\ell}(n)\bar{y}_{R,\ell}(n),\quad \bar{d}_{I,\ell}(n)=\bar{x}_{I,\ell}(n)\bar{y}_{I,\ell}(n), \quad (4)$$

$$\bar{x}_{R,\ell}(n)=0.5\left[3-\bar{y}_{R,\ell}^2(n)\right],\ \text{and}\ \bar{x}_{I,\ell}(n)=0.5\left[3-\bar{y}_{I,\ell}^2(n)\right]. \quad (5)$$

Replacing $d(n)-y(n)$ by $\bar{e}_k(n)$ in (1), we obtain DM-RMMA. To complete its derivation, the step-size $\tilde{\mu}$ should be chosen. To simplify the presentation, we assume real data.

If, at a certain iteration, $\|\mathbf{w}(n-1)\|$ is so large that $y^2(n)>3$ (note that $\sigma_a^2=1$), we can guarantee that DM-RMMA is stable by choosing $\tilde{\mu}$ as follows. Outside the region of interest, the update equation of DM-RMMA reduces to

$$\mathbf{w}(n)=\left[\mathbf{I}-\frac{\tilde{\mu}|c_k|}{\delta+\|\mathbf{u}(n)\|^2}\mathbf{u}(n)\mathbf{u}^T(n)\right]\mathbf{w}(n-1)+\frac{\tilde{\mu}|c_k|c_k\mathbf{u}(n)}{\delta+\|\mathbf{u}(n)\|^2}. \quad (6)$$

The matrix between brackets has all eigenvalues with absolute values less than or equal to one if [9]

$$0<\tilde{\mu}<2/|c_k|\le 2/|c_{\max}|, \quad (7)$$

where $c_{\max}$ is center of the region farther away from the origin of the complex plane of the M-QAM constellation. Note that $|c_{\max}|=\sqrt{2}(\sqrt{M}-2)$ for rectangular QAM. DM-RMMA can also be used to recover non-rectangular QAM. In this case, $|c_{\max}|\neq\sqrt{2}(\sqrt{M}-2)$.

The norm of the second term of the r.h.s. of (6) is bounded, i.e.,

$$0\le\frac{\tilde{\mu}|c_k|c_k\|\mathbf{u}(n)\|}{\delta+\|\mathbf{u}(n)\|^2}\le\frac{\tilde{\mu}|c_{\max}|c_{\max}}{\delta}<\infty. \quad (8)$$

Using (deterministic) exponential stability results for the LMS algorithm [9], we conclude that DM-RMMA is stable if $\tilde{\mu}$ is chosen in the interval (7). Although this result was obtained for real data, several simulations suggest that it can also be used for complex data.

DM-RMMA is summarized in Table 1. DM-RMMA requires only [$4\times$, $2+$, and $(\log_2 M-2)$ comparisons] per iteration in addition to DM-MMA.

Table 1. Summary of DM-RMMA

Initialize the algorithm by setting:

$\mathbf{w}(0)=[\,0\ \cdots\ 0\ \ 1+j\ \ 0\ \cdots\ 0\,]^T$; $0<\tilde{\mu}<2/|c_{\max}|$

for $n=1,2,\ldots$, compute:

$$y(n)=\mathbf{u}^T(n)\mathbf{w}(n-1) \quad (9)$$

Identify the region A_k, set $\alpha_k=1$, and compute:

$$\bar{y}_{R,k}(n)=y_R(n)-c_{R,k};\ \ \bar{y}_{I,k}(n)=y_I(n)-c_{I,k} \quad (10)$$

$$\bar{x}_{R,k}(n)=1.5-0.5\bar{y}_{R,k}^2(n);\ \ \bar{x}_{I,k}(n)=1.5-0.5\bar{y}_{I,k}^2(n) \quad (11)$$

if $\bar{x}_{R,k}(n)\ge 0$ and $\bar{x}_{I,k}(n)\ge 0$

$$\bar{d}_{R,k}(n)=\bar{x}_{R,k}(n)\bar{y}_{R,k}(n);\ \ \bar{d}_{I,k}(n)=\bar{x}_{I,k}(n)\bar{y}_{I,k}(n) \quad (12)$$

else

$$\bar{d}_{R,k}(n)=\bar{d}_{I,k}(n)=0; \quad (13)$$

end

$$\bar{e}_{R,k}(n)=\bar{d}_{R,k}(n)-\bar{y}_{R,k}(n);\ \ \bar{e}_{I,k}(n)=\bar{d}_{I,k}(n)-\bar{y}_{I,k}(n) \quad (14)$$

$$\bar{e}(n)=\alpha_k\left[|c_{R,k}|\bar{e}_{R,k}(n)+j|c_{I,k}|\bar{e}_{I,k}(n)\right] \quad (15)$$

$$\mathbf{w}(n)=\mathbf{w}(n-1)+\tilde{\mu}(\delta+\|\mathbf{u}(n)\|^2)^{-1}\,\bar{e}(n)\mathbf{u}^*(n) \quad (16)$$

end

To give further insight about the proposed algorithm, the error-functions of MMA, S-MMA, and RMMA are depicted in Fig. 1 for the real part of 64-QAM (the figure for the imaginary counterpart is identical). The error-function of MMA (resp., S-MMA) has zeros when y_R is null or when y_R^2 is equal (resp., close) to the dispersion constant. S-MMA exhibits increased contours in the error function, resulting in a smaller steady-state misadjustment than that of MMA [4]. For both MMA and S-MMA, the error-function is not zero when the equalizer output is equal to the symbol of the

nonconstant-modulus constellation. On the other hand, the error-function of RMMA presents nulls at the coordinates of the centers of each region A_k and at the coordinates of the symbols of the constellation. The nulls at the coordinates of the constellation symbols allow RMMA to treat nonconstant modulus signals as constant modulus signals.

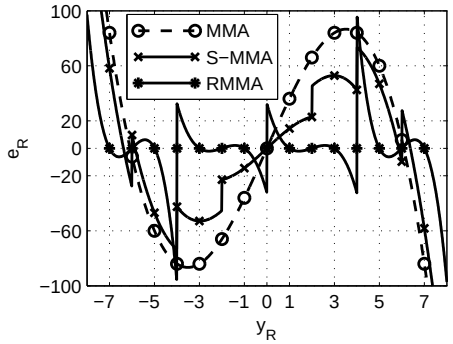

Fig. 1. Error-function for MMA, S-MMA, and RMMA, considering the real part of a 64-QAM constellation. RMMA plot scale 2.7:1, enlarged to ease zero-crossings visualization.

A drawback of DM-RMMA is that it still has the typical slow convergence of MMA. At the beginning of convergence, the coefficient vector $\mathbf{w}$ is very distant from the optimum solution, and the equalizer output often falls in a wrong region, mainly in the presence of noise. This wrong decision is fed back and the algorithm takes many iterations to converge. To improve its convergence, we have to take into account not only the region A_k, where the sample of equalizer output falls, but also the regions in its neighborhood. To avoid a large increase in the computational cost, we assume the influence of only K_r more regions besides A_k, as shown in Fig. 2-(a). Note that K_r can be equal to 2, 3, or 4, depending on the position of A_k. The factors α_ℓ of (2) must be nonzero for the K_r regions in the neighborhood of A_k. When the decision error $e_d(n) = \hat{a}(n-\Delta) - y(n)$ is large, the influence of the regions of the neighborhood in A_k should be greater than when $e_d(n)$ is small. With this in mind, we consider the mean-squared decision error estimated as $\xi(n) = \lambda\xi(n-1) + (1-\lambda)e_d^2(n)$, where $0 \ll \lambda < 1$ is a forgetting factor, and choose $\alpha_\ell = 4^{-p(n)}$, with $2 \le p(n) \le 10$ calculated through a hyperbolic tangent function, i.e.,

$$p(n) = 7.1467\frac{1-\mathrm{e}^{8[\xi(n)-0.03]}}{1+\mathrm{e}^{8[\xi(n)-0.03]}} + 9.1467. \qquad (17)$$

This function was experimentally chosen and is shown in Fig. 2-(b). Through simulations, we observe that the good behavior of the algorithm can be ensured with this function for different environments.

To distinguish this algorithm from that of Table 1, we denote it as DM-RMMA$_5$. Thus, after the identification of region A_k, Eqs. (10)-(14) of Table 1 should be evaluated for A_k and for K_r regions in its neighborhood. Then, (15) should be replaced by

$$\bar{e}(n) = \sum_{\ell=k}^{k+K_r} \alpha_\ell \left[|c_{R,\ell}|\bar{e}_{R,\ell}(n) + j|c_{I,\ell}|\bar{e}_{I,\ell}(n)\right] \qquad (18)$$

with $\alpha_\ell = \alpha_k = 1$ for the region A_k which contains the sample $y(n)$ and $\alpha_\ell = 4^{-p(n)}$ for the regions in the neighborhood of A_k.

Similarly to DM-RMMA, the step-size $\tilde{\mu}$ for DM-RMMA$_5$ should be chosen. Assuming again the real case, the update equation of DM-RMMA$_5$ outside the region of interest can be rewritten as

$$\mathbf{w}(n) = \left[\mathbf{I} - \frac{\tilde{\mu}\gamma}{\delta+\|\mathbf{u}(n)\|^2}\mathbf{u}(n)\mathbf{u}^T(n)\right]\mathbf{w}(n-1) + \frac{\tilde{\mu}\rho\mathbf{u}(n)}{\delta+\|\mathbf{u}(n)\|^2}. \qquad (19)$$

where $\gamma = |c_k| + 4^{-p(n)}\sum_{\ell=k}^{k+K_r}|c_\ell|$, and $\rho = c_k|c_k| + 4^{-p(n)}\sum_{\ell=k}^{k+K_r}c_\ell|c_\ell|$. The second term of the r.h.s. of (19) is bounded. Inspired in the results of [9], to ensure the stability of DM-RMMA$_5$, $\tilde{\mu}$ should be chosen in the interval

$$0 < \tilde{\mu} < 2/\gamma < 1.6/|c_{\max}|. \qquad (20)$$

In the worst case ($K_r = 4$), DM-RMMA$_5$ requires [$73\times$, $32+$, $8\div$, and 9 comparisons] per iteration in addition to DM-RMMA. To decrease the computational cost, DM-RMMA$_5$ can be switched to DM-RMMA when $\xi(n) \le 0.1$. Simulation results show that this switching does not cause a degradation of performance.

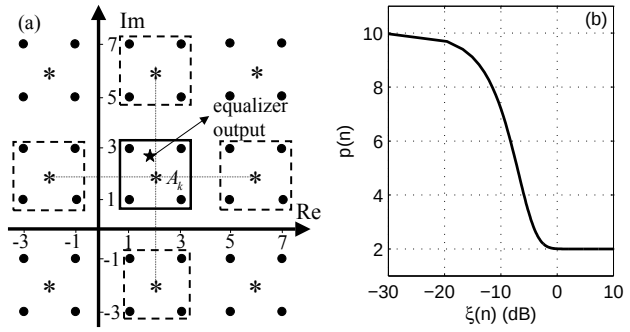

Fig. 2. (a) Local regions for RMMA adaptation ($K_r = 4$); the center of each local region is indicated by $*$, and the constellation symbols by $\bullet$; (b) the exponent $p(n)$ as a function of mean-squared decision error in dB.

4. SIMULATION RESULTS

DM-RMMA and DM-RMMA$_5$ are compared to DM-MMA and the Wiener solution. The equalizer has $N = 21$ taps and was initialized with the typical center spike in all simulations. Due to space reasons, the algorithms DM-MMA, DM-RMMA, and DM-RMMA$_5$ are denoted respectively as DM, R1-DM, and R5-DM in the legends of the figures. Furthermore, the following adaptation parameters were used in all simulations: $\mu_{DM-MMA} = 4\times10^{-3}$, $\mu_{DM-RMMA} = \mu_{DM-RMMA_5} = 10^{-2}$, and $\lambda = 0.9$. The delay of the Wiener filter was set to $\Delta = 11$. The step-sizes of the algorithms were chosen to obtain a tradeoff between convergence rate and steady-state misadjustment. In some cases, to facilitate the visualization, the curves were filtered by a moving-average filter with 500 taps.

Fig. 3-a shows the mean-squared decision error ($\mathrm{E}\{e_d^2(n)\}$) estimated from the ensemble-average of 200 independent runs. We assume 256-QAM, absence of noise, and that, at iteration $n = 2.5\times10^5$, the channel [0.28 0.92 0.28] is changed to [0.35 0.87 0.35]. DM-MMA presents a high misadjustment due to nonconstant modulus signals. DM-RMMA$_5$ and DM-RMMA outperform DM-MMA, converging to the Wiener solution. Although they achieve the same steady-state solution, DM-RMMA$_5$ converges faster than DM-RMMA, due to the use of the regions in the neighborhood of A_k. Fig. 3-b shows the ensemble-average of the exponent $p(n)$. When $p(n) \approx 10$, DM-RMMA$_5$ could be switched to DM-RMMA without performance degradation.

Fig. 4 shows the symbol error rate (SER) as a function of the signal-to-noise ratio (SNR). We assume the channel [0.28 0.92 0.28], 256-QAM (Fig. 4-a), and 1024-QAM (Fig. 4-b). For 256-QAM, the performance of DM-RMMA$_5$ is close to that of the Wiener filter, outperforming DM-MMA, whose SER tends to 10^{-3}. For 1024-QAM, DM-MMA presents a SER lower-bounded by 10^{-1}. For SNR < 32 dB, the algorithms and the Wiener filter present a high SER and can not be used in practical situations. For $32 <$ SNR $<$ 38 dB, DM-RMMA$_5$ is outperformed by DM-MMA, however, this

behavior could be improved if more regions in the neighborhood of A_k were taken into account, since for low SNR, the equalizer output can fall in a wrong region with high probability. Possibly, to take the estimate of the coefficient vector closer to the Wiener solution, the number of regions in the neighborhood of A_k should be increased for low SNR. This disadvantage occurs only for high SER values ($>10^{-1}$), at which the equalizers would be useless. For $\mathrm{SNR} > 38$ dB, DM-RMMA$_5$ gets close to the Wiener filter. It should be noticed that, in practical situations, uncoded 1024-QAM signals require $\mathrm{SNR} > 40$ dB for attaining SER $< 10^{-7}$.

Fig. 5 shows $e_d^2(n)$ assuming the time-variant channel $H(z,n) = 1 + z^{-11}0.008\sin(2 \times 10^{-5}\pi n)$, absence of noise, and 1024-QAM. DM-RMMA$_5$ tracks the channel variation, presenting $e_d^2(n)$ at least 10 dB lower than that of DM-MMA, which does not converge. DM-RMMA converges only around $n = 5.8 \times 10^5$, afterwards following DM-RMMA$_5$.

To show the robustness of DM-algorithms, Fig. 6 shows $e_d^2(n)$, under a disturbed received signal, assuming the channel [0.28 0.92 0,28], absence of noise, and 256-QAM. At iterations 1.25×10^5 and 2.5×10^5, the received signal is disturbed by a spike with amplitude 10^{10}. All the algorithms do not diverge. DM-MMA converges for a moderate level of $e_d^2(n)$ only after the second spike. DM-RMMA converges to the same level of $e_d^2(n)$ of that of DM-RMMA$_5$, but after a large number of iterations.

5. CONCLUSION

We have proposed an algorithm for blind equalization of high-order QAM signal. The simulation results show that the proposed algorithm presents a stable behavior and converges approximately to the Wiener solution. A proof of the return to the region of interest and the stability analysis for the complex case are under research. It should be stressed that the behavior of the proposed algorithm for 1024-QAM signals is worse than that of the DM-MMA for low SNR values, but this situation can be improved by considering additional neighbors. New studies are being carried on in this direction, considering also different channels. Finally, it is important to emphasize that the idea presented here can be extended to other blind algorithms such as SWA.

6. REFERENCES

[1] C. R. Johnson Jr. *et al.*, "Blind equalization using the constant modulus criterion: a review," *Proc. IEEE*, vol. 86, pp. 1927–1950, Oct. 1998.

[2] K. N. Oh and Y. O. Chin, "Modified constant modulus algorithm: Blind equalization and carrier phase recovery algorithm," in *Proc. of IEEE Int. Conf. Commun.*, 1995, vol. 1, pp. 498–502.

[3] J. Yang, J.-J. Werner, and G. A. Dumont, "The multimodulus blind equalization and its generalized algorithms," *IEEE J. Sel. Areas Commun.*, vol. 20, pp. 997–1015, Jun. 2002.

[4] S. Abrar and R. A. Axford Jr., "Sliced multi-modulus blind equalization algorithm," *ETRI Journal*, vol. 27, pp. 257–266, Jun. 2005.

[5] S. Chen, "Low complexity concurrent constant modulus algorithm and soft directed scheme for blind equalization," *IEE Proc. Vis., Image, Signal Process.*, vol. 150, pp. 312–320, Oct. 2003.

[6] M. T. M. Silva and V. H. Nascimento "Stochastic Stability Analysis for the Constant-Modulus Algorithm," *IEEE Trans. Signal Process.*, vol. 56, pp. 4984–4989, Oct. 2008.

[7] M. D. Miranda, M. T. M. Silva, and V. H. Nascimento, "Avoiding divergence in the Constant Modulus Algorithm," in *Proc. of ICASSP'08*. IEEE, 2008, pp. 3565–3568.

[8] M. D. Miranda, M. T. M. Silva, and V. H. Nascimento, "Avoiding divergence in the Shalvi Weinstein Algorithm," *IEEE Trans. Signal Process.*, vol. 56, pp. 5403–5413, Nov. 2008.

[9] Vítor H. Nascimento, *Stability and Performance of Adaptive Filters without Slow Adaptation Approximations*, Ph.D. thesis, University of California, Los Angeles, 1999.

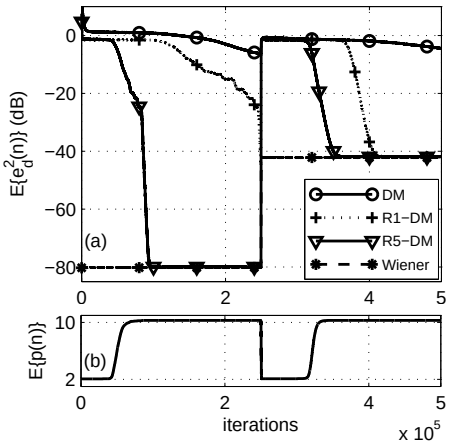

Fig. 3. (a) $\mathrm{E}\{e_d^2(n)\}$ for DM-MMA, DM-RMMA, DM-RMMA$_5$. (b) $\mathrm{E}\{p(n)\}$; 256-QAM; ensemble average of 200 runs.

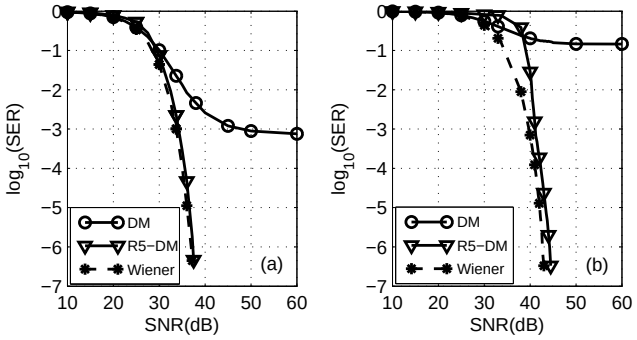

Fig. 4. Log of SER as a function of SNR for (a) 256-QAM (b) 1024-QAM.

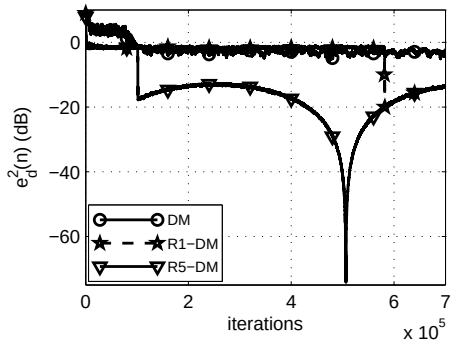

Fig. 5. Squared decision error; time-variant channel, and 1024-QAM.

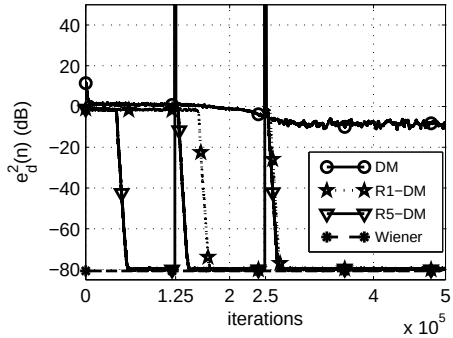

Fig. 6. Squared decision error; $u(1.25 \times 10^5) = u(2.5 \times 10^5) = 10^{10}$ for 256-QAM.